

An Efficient Dual-Circularly Polarized Rectenna for RF Energy Harvesting in the 2.45 GHz ISM Band

Walid Haboubi¹, Hakim Takhedmit^{1, *}, Jean-Daniel Lan Sun Luk²,
Salah-Eddine Adami³, Bruno Allard³, François Costa⁴,
Christian Vollaire³, Odile Picon¹, and Laurent Cirio¹

Abstract—This paper reports a 2.45 GHz, low power dual circularly polarized (DCP) and dual access rectenna. It contains two dc-recombined rectifiers and a cross-slot coupled square patch antenna fed by a microstrip line. A judicious dc recombination scheme allows to minimize the RF power imbalance between accesses caused by multipath effects and consequently arbitrary polarized incident waves. The proposed rectenna is then able to harvest linearly polarized, right-hand circularly polarized (RHCP) and left-hand circularly polarized (LHCP) electromagnetic waves, with nearly stable performances. The rectenna has been optimized at -15 dBm per access and dedicated to remote and contactless supply low consumption sensors. It has been experimentally tested with very low power densities from $0.057 \mu\text{W}/\text{cm}^2$ ($E_{rms} = 0.46$ V/m) to $2.3 \mu\text{W}/\text{cm}^2$ ($E_{rms} = 2.95$ V/m). At $1.49 \mu\text{W}/\text{cm}^2$ (-15 dBm on each rectifier), the structure exhibits an output dc voltage and a global efficiency of 189 mV and 37.7%, respectively when the azimuthal angle (Φ) of the incident field is equal to 0° . Due to the nearly constant total gain of the DCP antenna and an appropriate dc recombination of the two rectifiers, the global efficiency slightly varies between 37.7% and 41.4% when the azimuthal angle (Φ) varies between -90 and 90° .

1. INTRODUCTION

In the context of electromagnetic energy harvesting applications [1–3] for low consumption wireless sensors or sensor networks, many rectennas have been developed within the last few years. The rectenna is an essential device to collect electromagnetic RF power through free space and convert it into useful dc power. It contains a receiving antenna and RF-to-dc rectifier. The rectifier is often made up of a combination of Schottky diodes, an input HF filter and an output bypass capacitor. A load resistor, connected at the output of the rectifier, represents the input impedance of the device to be powered. The input HF filter, localized between the antenna and diodes, acts as a low-pass filter that rejects harmonics generated by the diodes. It also ensures an impedance matching between the two parts of the rectenna [4, 5]. Indeed, for a given input RF power level, the conversion efficiency is mainly affected by the diode losses and the impedance mismatching.

The microwave converter can take several topologies. The single series [5–7] and shunt [4, 8] configurations are the most used. The voltage doubler [4, 9, 10] topology is also used to enhance the output dc voltage level.

In ambient energy harvesting scenario, the incoming incident fields on the rectenna have an unknown angle of incidence. This is mainly due to the specific characteristic of an indoor [11] or urban

Received 11 March 2014, Accepted 16 April 2014, Scheduled 27 June 2014

* Corresponding author: Hakim Takhedmit (hakim.takhedmit@u-pem.fr).

¹ ESYCOM Laboratory, Université Paris-Est, EA2552, UPEMLV, Champs-sur-Marne 77454, France. ² LE2P Laboratory, Université de la Réunion, EA4079, Faculté des Sciences et Technologies, 15, Avenue René Cassin BP7151, Saint Denis, Iles de la Réunion 97715, France. ³ AMPERE Laboratory, UMR 5005, EC-INSA Lyon, Lyon 69130, France. ⁴ SATIE Laboratory, UMR 8029, ENS Cachan, Cachan 94235, France.

environment, where multipath effects can cause depolarization phenomenon. Circularly polarized (CP) rectenna with a single access [4, 12, 13] were proposed to provide a nearly constant output dc voltage regardless to the electric-field angle of incidence. However, in the case of a CP rectenna illuminated by a linearly polarized incident field, a well-known 3-dB polarization mismatch appears and decreases the amount of RF power that can be collected by the antenna. The use of two rectennae with orthogonal polarizations can solve this problem. Nevertheless, this increases the geometrical dimensions of the structure. Another solution consists in developing two co-localized orthogonally polarized antennas on the same substrate. In [14], an array of dual linearly polarized rectennas fed by a coupling slot was studied to wirelessly supply actuators. The structure was optimized for high power densities up to $38.8 \mu\text{W}/\text{cm}^2$. In [15], an antenna with dual linear polarizations was reported. Both antenna accesses were connected to a voltage doubler circuit, and recombined on a common dc resistive load. The output dc voltage exhibits a large ripple of 2.33 dB when the angle of the incident electric field varies between 0 and 360° . In [16], a 2.45-GHz CP shorted-ring slot antenna associated with a series diode rectifier was proposed. It exhibits a measured axial ratio (AR) of 1.52 dB and an efficiency ripple ($\Delta\eta$) of 0.91 dB. The efficiency ripple represents the difference between the maximum and minimum of the output dc power, when the azimuthal angle Φ varies.

A CP patch rectenna with harmonic suppression and a dc voltage doubler was reported in [17]. The CP property was obtained by introducing two peripheral cuts. It shows a measured AR of 0.9 dB at 2.45 GHz and an efficiency ripple of 1.66 dB.

A 5.8-GHz CP truncated corner square patch microstrip antenna combined with a coplanar stripline (CPS) rectifier was proposed in [18] for microwave power transmission applications. A 0.3-dB axial ratio was obtained with an efficiency ripple of 0.42 dB.

This paper proposes a dual circularly polarized (DCP) rectenna and dual accesses able to capture Left Hand Circularly Polarized (LHCP), Right Hand Circularly Polarized (RHCP) and linearly polarized waves. Both accesses are connected to a microwave rectifier and dc power is recombined on a common resistive load. This avoids the 3-dB polarization mismatch encountered when CP rectennas are used to harvest linearly polarized waves. The antenna part is fed by coupling technique [19] with a cross-slot etched on the ground plane. It has been characterized in term of gain and power imbalance between accesses. Unlike the previous study presented in [20] with results mainly focused on the antenna issue, a particular attention was given to the dc recombination scheme to significantly reduce the efficiency ripple when an arbitrary (circularly, linearly) polarized wave illuminates the rectenna. In addition, the rectifier part has been optimized at very low power densities of -15 dBm per access instead of 10 dBm like in [20].

The rectenna, including antenna and rectifier, has been experimentally evaluated in terms of global conversion efficiency and output dc voltage, for several azimuthal angles.

2. ANTENNA CHARACTERISTICS

The DCP antenna depicted in Fig. 1 was optimized using Ansoft HFSS [21]. The square patch antenna is printed on a 3.175-mm thick Duroid 5880 ($\epsilon_r = 2.2$) at the upper substrate. The $50\text{-}\Omega$ microstrip feeding line is printed on a 1.524-mm thin Arlon 25N substrate ($\epsilon_r = 3.4$) at the lower layer of the antenna. A crossed coupling slot is etched on the ground plane and is accurately adjusted below the square patch to maximize the coupling at 2.45 GHz and to mismatch the antenna and reject the 4.9-GHz second harmonic. The antenna was fabricated and experimentally characterized inside an anechoic chamber. Geometrical dimensions are summarized in Fig. 1.

Figure 2 shows the antenna linear gains evolution measured per access. The experiments have been performed in an anechoic chamber by illuminating the antenna under test with a linearly polarized electromagnetic wave at 2.45 GHz from a transmitting horn antenna. At boresight (elevation angle $\theta = 0^\circ$), the gain per access is deduced from the output power measured in one access when the azimuthal angle (Φ) of the incident electric field varies. The second access is terminated on a $50\text{-}\Omega$ matched load. As shown in Fig. 2, the maximum gain imbalance between both accesses is 2.8 dB. At $\Phi = 0^\circ$, the gains are equal because the antenna is symmetrically illuminated. The total gain is calculated from the total power received on the left and the right accesses and is depicted on Fig. 2. A maximum total gain of 6.4 dBi is obtained at $\Phi = -90^\circ$ and a minimum of 5.5 dBi is obtained at

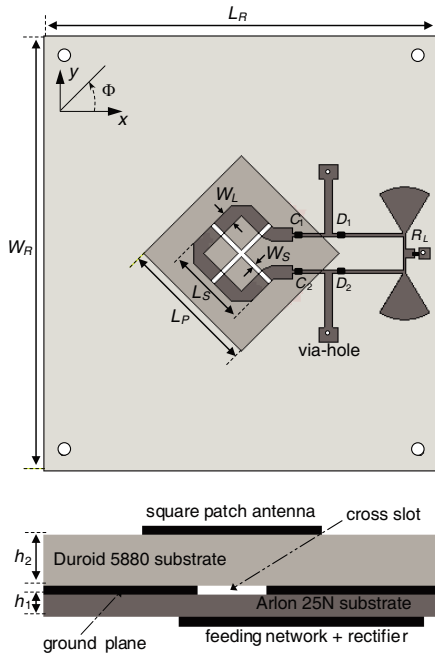


Figure 1. Layout of the proposed rectenna. $L_R = 100$, $W_R = 110$, $L_P = 34.8$, $L_S = 20.45$, $W_L = 3.45$, $W_S = 1.25$, $h_1 = 1.524$, $h_2 = 3.175$ (all dimensions are in millimeter).

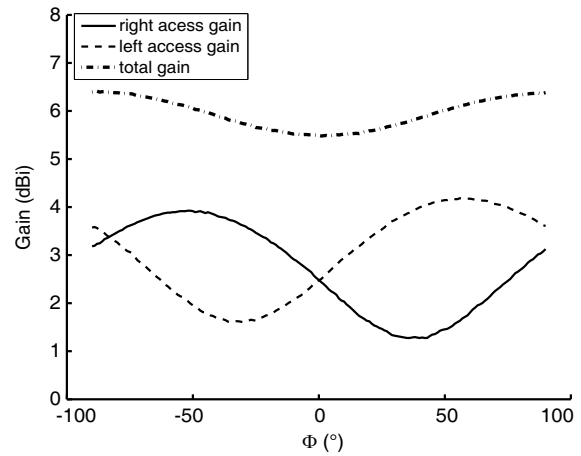


Figure 2. Experimental gains (per access and total) of the DCP antenna versus azimuthal angle (Φ).

$\Phi = 0^\circ$, resulting in a total-gain ripple of 0.9 dB. When Φ varies, a decrease of the gain on an access is substantially compensated by the gain on the other access resulting in a stable and nearly constant total gain.

3. RF-to-dc CONVERSION CIRCUIT

3.1. Series and Parallel Interconnection Topologies

As previously mentioned, an appropriate dc recombination is essential to reduce the effects of a power imbalance on the conversion efficiency (η). Here, the rectifiers of the DCP rectenna can be interconnected in series or in parallel (Fig. 3) [4]. These recombination schemes were simulated using Harmonic Balance [22] of Agilent ADS (Advanced Design System), considering a -15 dBm input RF power on each

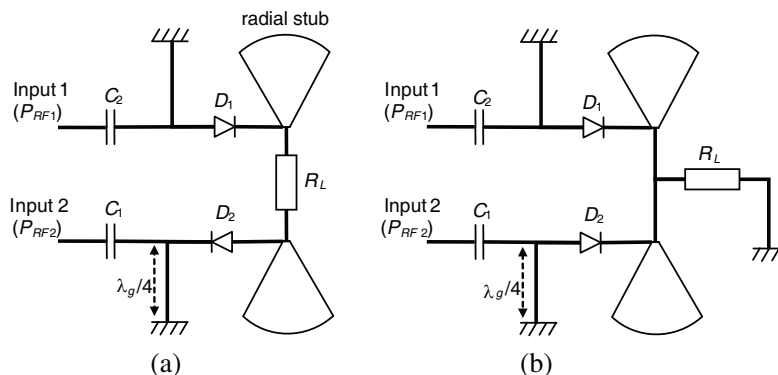


Figure 3. (a) Series and (b) parallel recombination topologies.

access. The rectifier is based on Skyworks SMS 7630-079LF Schottky diodes on a SC-79 packages [23] for very low power level considerations. The design has been optimized to maximize the RF-to-dc conversion efficiency. The optimal dc load of the single rectifier is equal to $3\text{ k}\Omega$ at -15 dBm RF power.

For the series recombination (Fig. 3(a)), the dc load is twice higher ($R_L = 6\text{ k}\Omega$). The same dc current flows through the diodes (D_1 and D_2) and the resistive load R_L . The voltage is measured over the load without reference to the ground plane. One diode provides a positive dc voltage and the second provides a negative dc voltage.

For the parallel recombination (Fig. 3(b)), the dc load is divided by 2 ($R_L = 1.5\text{ k}\Omega$) in comparison with the single rectifier. The dc currents flowing in the two rectifiers are different except in the case of a balanced RF power on each access. These currents are recombined on a resistive load localized between the output of the rectifiers and the ground plane.

Figure 4(a) shows the ADS simulated RF-to-dc conversion efficiency versus P_{RF1} and P_{RF2} in the series recombination case. The efficiency decreases significantly when an imbalance between accesses exists. From 56.5% in the balanced case ($P_{RF1} = P_{RF2} = -10\text{ dBm}$), the efficiency drops to 39.7% when $P_{RF1} = -10\text{ dBm}$ and $P_{RF2} = -50\text{ dBm}$.

In the parallel recombination case (Fig. 4(b)), the RF-to-dc conversion efficiency also decreases when an RF imbalance occurs but in a more slightly way. Indeed, from 56.7% in the balanced case ($P_{RF1} = P_{RF2} = -10\text{ dBm}$), the efficiency drops to 47.4% when $P_{RF1} = -10\text{ dBm}$ and $P_{RF2} = -50\text{ dBm}$. The parallel recombination is less sensitive to power imbalances and is then more suitable when circularly polarized or linearly polarized waves with arbitrary angle of incidence are considered. Further details about this topology will be given in the next section.

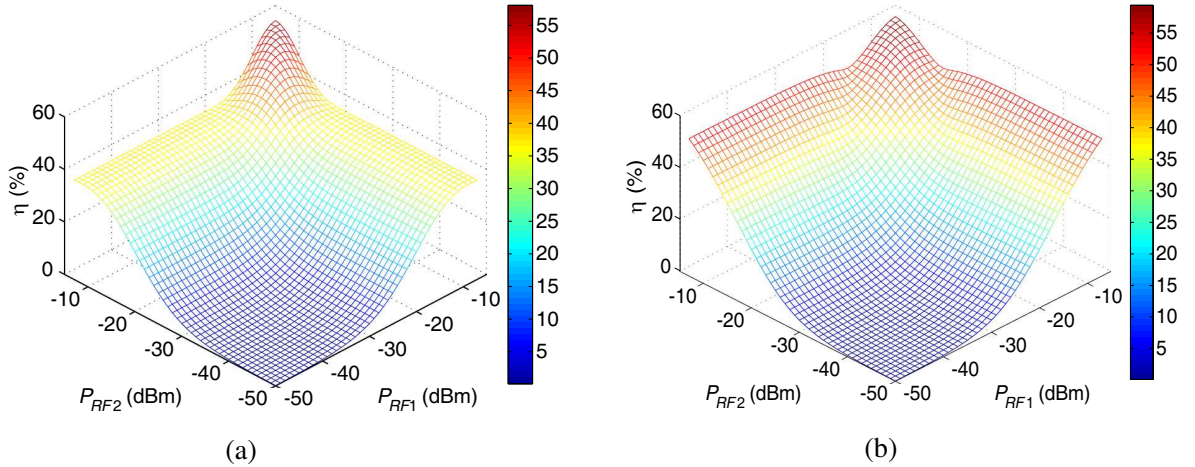


Figure 4. RF-to-dc conversion efficiency versus P_{RF1} and P_{RF2} . (a) In the series topology. (b) In the parallel topology.

3.2. Description of the Rectifier Design

The parallel interconnected rectifier has been accurately designed and optimized using Agilent ADS. Firstly, the distributed part of the circuit was simulated using ADS Momentum and then the scattering parameters were extracted. Secondly, Harmonic Balance uses these parameters and the packaged lumped elements models to simulate the complete design.

The circuit doesn't include an input HF filter. The impedance mismatching between the DCP antenna and the rectifier at 4.9 and 7.35 GHz harmonics has been evaluated [24]. Besides, the HFSS-simulated input impedance of the receiving antenna at the fundamental and two high-order harmonics (see Table 1) were taken into account in ADS simulations.

The total length of the parallel rectifier is 35 mm and is printed on the Arlon 25N lower substrate layer. Details of the optimized dimensions are given in Fig. 5.

Table 1. Antenna input impedance.

| Frequency (GHz) | Resistance (Ω) | Reactance (Ω) |
|-----------------|-------------------------|------------------------|
| 2.45 | 58.8 | -15.5 |
| 4.9 | 6.3 | -38.6 |
| 7.35 | 156 | -58.2 |

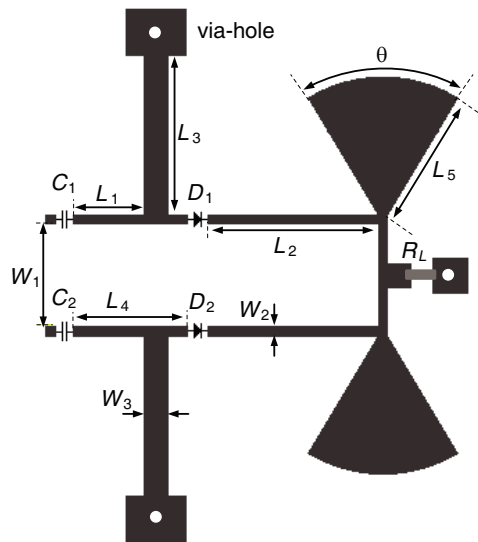


Figure 5. Rectifier Layout ($L_1 = 6.2$, $L_2 = 14.8$, $L_3 = 15$, $L_4 = 10$, $L_5 = 11.5$, $W_1 = 8.65$, $W_2 = 0.8$, $W_3 = 2$, $\theta = 62^\circ$) (all dimensions are in millimeter).

At the input of each rectifier, a surface-mount capacitor (C_1, C_2) of 15 pF is foreseen to stop the dc current flowing towards the antenna. A short-circuited parallel stub of 15 mm length and 2 mm width is connected to the microstrip feeding line for the dc path and also to adjust the impedance matching between the rectifier and the antenna. To suppress the 2.45 GHz RF component over the load, a radial stub (L_5 , sectoral angle θ) has been used. In addition, a microstrip line between the radial stub and the Schottky diode is accurately tuned ($L_2 = 14.8$ mm) to reduce the reactance of the diode ($Z_{diode} = 50.5 - j318.6 \Omega$) computed at -15 dBm RF power. Furthermore, the input impedance of the diode computed between the anode and the ground plane is $53 - j67 \Omega$. Due to the matching network, the impedance at the input of the rectifier is then $53 + j6 \Omega$. The simulated optimal load is $1.5 \text{ k}\Omega$ considering -15 dBm on each access. The corresponding RF-to-dc conversion efficiency is 43.5% and increases up to 54.5% for a maximum input power of -5 dBm per access. The low reverse breakdown voltage ($V_{br} = 2 \text{ V}$) of the diode limits the amount of RF power that can be converted [25].

4. EXPERIMENTAL CHARACTERIZATION OF THE RECTENNA

The proposed dual circularly polarized rectenna has been fabricated (see Fig. 6) and experimentally characterized inside an anechoic chamber using the measurement setup shown in Fig. 7. A 37-dB gain power amplifier connected between the RF generator and the horn antenna was used. The distance between the transmitting horn antenna ($G_t = 12.2 \text{ dBi}$) and the rectenna is 1 meter. Then, the rectenna is localized in the far field horn antenna's zone ($D > 0.5 \text{ m}$) and illuminated at its broadside ($\theta = 0^\circ$).

The dc resistive load is connected at the output of the rectifier. Before starting measurements, the rectenna has been calibrated and illuminated at $\Phi = 0^\circ$ to obtain -15 dBm on each access. This corresponds to an incident power density of $1.49 \mu\text{W}/\text{cm}^2$ on the antenna. The conversion efficiency is

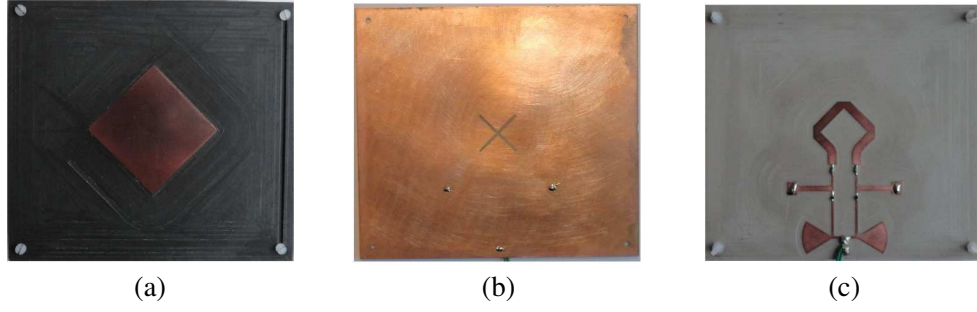


Figure 6. Picture of the proposed rectenna. (a) Patch antenna. (b) Cross-slot etched in the ground plane. (c) RF-to-dc rectifying circuit.

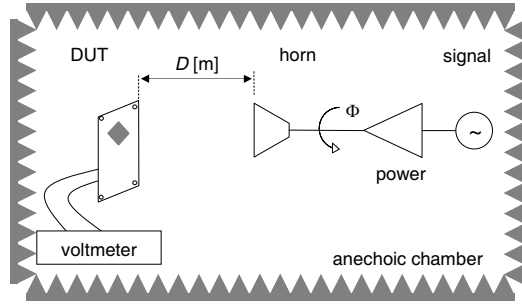


Figure 7. Measurement setup.

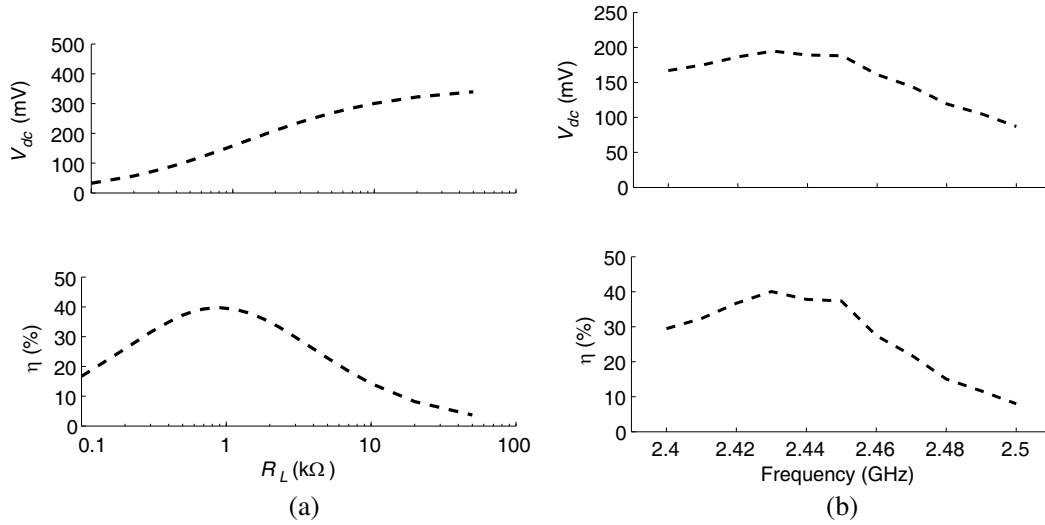


Figure 8. Measured output dc voltage and efficiency (a) against output load R_L ($f = 2.45$ GHz, $\Phi = 0^\circ$). (b) Against frequency ($R_L = 1.5$ k Ω , $\Phi = 0^\circ$).

computed using:

$$\eta = 100 \times \frac{P_{DC}}{P_{RF}} = 100 \times \frac{V_{dc}^2}{R_L S_{eff}(\Phi) \rho_{RF}} \quad (1)$$

where V_{dc} is the measured output dc voltage, ρ_{RF} the incident RF power density, and $S_{eff}(\Phi)$ the effective aperture of the antenna, which depends on the total gain and the azimuthal angle Φ as shown in Fig. 2.

Figure 8(a) exhibits the measured output dc voltage and efficiency when the resistive load varies

from 0.1 to 50 kΩ at 2.45 GHz. The azimuthal angle (Φ) and the power density are set to 0° and 1.49 μW/cm² ($E_{rms} = 2.37$ V/m), respectively. Results show that the output dc voltage increases as the load value increases. The maximum efficiency is obtained for an optimal load close to 1.5 kΩ, which is in good concordance with simulations.

Figure 8(b) shows the measured output dc voltage and efficiency of the rectenna when frequency varies from 2.4 to 2.5 GHz. The RF power and the output load are set to -15 dBm per access and 1.5 kΩ, respectively. Results show a maximum dc output voltage and efficiency close to 2.45 GHz.

The variation of measured output dc voltage and efficiency, when the azimuthal angle (Φ) varies from -90 up to 90°, for a power density of 1.49 μW/cm², is depicted on Fig. 9, for a power density of 1.49 μW/cm². The efficiency is nearly constant and comprised between 37.7% ($\Phi = 0^\circ$) and 41.4% ($\Phi = -45^\circ$) with a very low efficiency ripple of 0.4 dB. As previously mentioned about the rectifier part, these results show that the proposed rectenna is able to capture and convert RF power, regardless the polarization of the incident electromagnetic wave.

The measured output dc voltage and conversion efficiency as a function of power density when the rectenna is rotated in the azimuthal plane ($\Phi = -90^\circ, -45^\circ, 0^\circ, 45^\circ, 90^\circ$) are depicted in Figs. 10(a) and 10(b), respectively. The rectenna is illuminated at its broadside using a linearly polarized horn

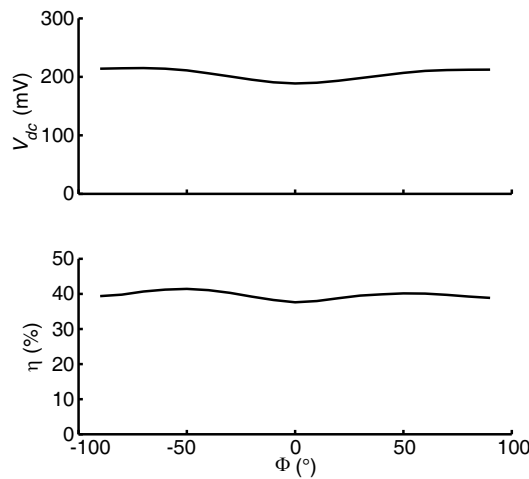


Figure 9. Measured output dc voltage and conversion efficiency versus azimuthal angle ($\rho_{RF} = 1.49 \mu\text{W}/\text{cm}^2$, $f = 2.45$ GHz).

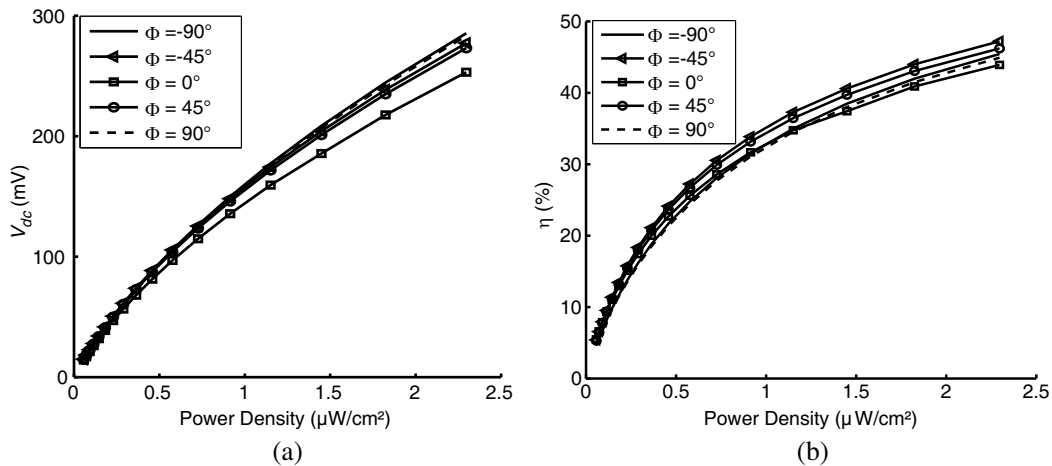


Figure 10. Measured (a) output voltage and (b) global conversion efficiency of the rectenna ($f = 2.45$ GHz, $R_L = 1.5$ kΩ).

antenna giving an incident RF power density on the rectenna from $0.057 \mu\text{W}/\text{cm}^2$ ($E_{rms} = 0.46 \text{ V/m}$) to $2.3 \mu\text{W}/\text{cm}^2$ ($E_{rms} = 2.95 \text{ V/m}$).

The output dc voltage and conversion efficiency increase when the power density increases. At $1.49 \mu\text{W}/\text{cm}^2$ (-15 dBm at the input of each rectifier), the measured output voltage and global efficiency are respectively 189 mV and 37.7% at $\Phi = 0^\circ$.

For the same power density and when the polarization angle varies, the output dc voltage is comprised between 189 mV and 215 mV and the global conversion efficiency varies between 37.7% and 41.4% . Therefore, the corresponding output dc power slowly evolves between $23.8 \mu\text{W}$ and $30.5 \mu\text{W}$ over an optimal $1.5 \text{ k}\Omega$ resistive load.

At $0.23 \mu\text{W}/\text{cm}^2$ (-23 dBm on each rectifier) and $\Phi = 0^\circ$, the dc voltage and efficiency are 46.9 mV and 15% , respectively. Similarly, at $2.3 \mu\text{W}/\text{cm}^2$ (-13 dBm on each rectifier), the dc voltage and efficiency rise to 253 mV and 43.9% , respectively.

In the power density range, all the measured curves in Fig. 10(b) are slightly similar. The 3-dB polarization mismatch, usually observed when dealing with CP rectennas, is overcome by the proposed dual circularly polarized antenna. In addition, the parallel dc recombination reduces the efficiency ripple that could be increased by power imbalance between accesses.

5. CONCLUSION

A low power dual circularly polarized rectenna in the 2.45 GHz ISM band has been investigated in this paper. The co-localized dual circularly polarized properties of the antenna avoid the well-known 3 dB polarization mismatch when the structure is illuminated by a linearly polarized wave. It was shown that the parallel recombination scheme minimizes the effects of a power imbalance. Experimental results show a very low ripple of the output dc voltage and the global conversion efficiency when the azimuthal angle varies. In this paper, the rectifier was optimized for -15 dBm per access. An output dc voltage and global efficiency of 215 mV and 41.4% , at $1.49 \mu\text{W}/\text{cm}^2$ ($E_{rms} = 2.37 \text{ V/m}$) very low RF power density have been measured.

The rectenna allows to harvest RHCP, LHCP and linearly polarized electromagnetic waves. It is particularly suitable for remote power supply such as low-power-consumption sensors and sensor nodes by recycling RF ambient energy.

ACKNOWLEDGMENT

This work is supported by the ANR (Agence Nationale de la Recherche) through the project REC-EM ANR-10-BLAN-0906.

REFERENCES

1. Paing, T., J. Morroni, A. Dolgov, J. Shin, J. Brannan, R. Zane, and Z. Popovic, "Wirelessly-powered wireless sensor platform," *Proc. of the 37th European Microw. Conference*, Munich, 999–1002, Oct. 2007.
2. Olgun, U., C.-C. Chen, and J. L. Volakis, "Design of an efficient ambient WiFi energy harvesting system," *IET Microw. Antennas Propag.*, Vol. 6, No. 11, 1200–1206, 2012.
3. Hong, S. S. B., R. Ibrahim, M. H. M. Khir, H. Daud, and M. A. Zakariya, "Rectenna architecture based energy harvester for low power RFID applications," *4th International Conference on Intelligent and Advanced Systems (ICIAS)*, 382–387, Petronas, Malaysia, Jun. 12–14, 2012.
4. Ren, Y. J. and K. Chang, "5.8-GHz circularly polarized dual-diode rectenna and rectenna array for microwave power transmission," *IEEE Trans. Microw. Theory Tech.*, Vol. 54, No. 4, 1495–1502, Apr. 2006.
5. Douyere, A., J. D. Lan Sun Luk, and F. Alicalapa, "High efficiency microwave rectenna circuit: Modeling and design," *Electronics Letters*, Vol. 44, No. 24, 1409–1410, Nov. 2008.
6. Zbitou, J., M. Latrach, and S. Toutain, "Hybrid rectenna and monolithic integrated zero-bias microwave rectifier," *IEEE Trans. on Microw. Theory and Tech.*, Vol. 54, No. 1, 147–152, Jan. 2006.

7. Monti, G., L. Corchia, and L. Tarricone, "ISM band rectenna using a ring loaded monopole," *Progress In Electromagnetics Research C*, Vol. 33, 1–15, 2012.
8. Strassner, B. and K. Chang, "5.8-GHz circularly polarized rectifying antenna for wireless microwave power transmission," *IEEE Trans. on Microw. Theory and Tech.*, Vol. 50, No. 8, 1870–1876, Aug. 2002.
9. Heikkinen, J. and M. Kivikoski, "Low-profile circularly polarized rectifying antenna for wireless power transmission at 5.8 GHz," *IEEE Microw. Wireless Compon. Lett.*, Vol. 14, No. 4, 162–164, Apr. 2004.
10. Heikkinen, J. and M. Kivikoski, "A novel dual-frequency circularly polarized rectenna," *IEEE Antennas Wireless Propag. Lett.*, Vol. 2, 330–333, 2003.
11. Perez-Vega, C. and J. L. Garcia, "Polarisation behaviour in the indoor propagation channel," *Electronics Letters*, Vol. 33, No. 10, 898–899, Mar. 1997.
12. Ali, M., G. Yang, and R. Dougal, "Miniature circularly polarized rectenna with reduced out-of-band harmonics," *Antennas and Wireless Propag. Lett.*, Vol. 5, 107–110, 2006.
13. Yo, T. C., C. M. Lee, C. M. Hsu, and C. H. Luo, "Compact circularly polarized rectenna with unbalanced circular slots," *IEEE Trans. Antennas Propag.*, Vol. 56, No. 56, 882–886, Mar. 2008.
14. Epp, L. W., A. R. Khan, H. K. Smith, and R. P. Smith, "A compact dual-polarized 8.51 GHz rectenna for high-voltage (50 V) actuator applications," *IEEE Trans. Microw. Theory Tech.*, Vol. 48, No. 1, 111–120, Jan. 2000.
15. Georgiadis, A., G. Andia, and A. Collado, "Rectenna design and optimization using reciprocity theory and harmonic balance analysis for electromagnetic (EM) energy harvesting," *IEEE Antennas and Wireless Propag. Lett.*, Vol. 9, 444–446, 2010.
16. Takhedmit, H., L. Cirio, S. Bellal, D. Delcroix, and O. Picon, "Compact and efficient 2.45 GHz circularly polarised shorted ring-slot rectenna," *Electronics Letters*, Vol. 48, No. 5, 253–254, 2012.
17. Huang, F.-J., T.-C. Yo, C.-M. Lee, and C.-H. Luo, "Design of circular polarization antenna with harmonic suppression for rectenna application," *IEEE Antennas and Propagation Letters*, Vol. 11, 592–595, 2012.
18. Hao, H. and K. Li, "A novel 5.8 GHz circularly polarized rectenna for microwave power transmission," *Proceed. of the 7th International Symposium on Antennas, Propagation & EM Theory, ISAPE'06*, 1–4, Guilin, China, Oct. 26–29, 2006.
19. Sullivan, P. L. and D. H. Schaubert, "Analysis of an aperture coupled microstrip antenna," *IEEE Trans. on Antennas and Propag.*, Vol. 34, No. 8, 977–984, Aug. 1986.
20. Harouni, Z., L. Cirio, L. Osman, A. Gharsallah, and O. Picon, "A dual circularly polarized 2.45-GHz rectenna for wireless power transmission," *IEEE Antennas and Wireless Propag. Lett.*, Vol. 10, 306–309, 2011.
21. Ansoft Corporations, "HFSS V.11 — Software based on the finite element method,".
22. "The advanced design system," Available: http://www.ece.uci.edu/eceware/ads_docs/.
23. Datasheet Skyworks: Surface Mount Mixer and Detector Schottky Diodes (SMS 7630-079LF).
24. Takhedmit, H., L. Cirio, O. Picon, C. Vollaire, B. Allard, and F. Costa, "Design and characterization of an efficient dual patch rectenna for microwave energy recycling in the ISM band," *Progress In Electromagnetics Research C*, Vol. 43, 93–108, 2013.
25. Yoo, T.-W. and K. Chang, "Theoretical and experimental development of 10 and 35 GHz rectennas," *IEEE Trans. Microw. Theory Tech.*, Vol. 40, No. 6, 1259–1266, Jun. 1992.